RSC Advances

This is an *Accepted Manuscript*, which has been through the Royal Society of Chemistry peer review process and has been accepted for publication.

Accepted Manuscripts are published online shortly after acceptance, before technical editing, formatting and proof reading. Using this free service, authors can make their results available to the community, in citable form, before we publish the edited article. This *Accepted Manuscript* will be replaced by the edited, formatted and paginated article as soon as this is available.

You can find more information about *Accepted Manuscripts* in the Information for Authors.

Please note that technical editing may introduce minor changes to the text and/or graphics, which may alter content. The journal's standard Terms & Conditions and the Ethical guidelines still apply. In no event shall the Royal Society of Chemistry be held responsible for any errors or omissions in this *Accepted Manuscript* or any consequences arising from the use of any information it contains.

ROYAL SOCIETY OF CHEMISTRY

www.rsc.org/advances

Journal Name

ARTICLE TYPE

Cite this: DOI: 10.1039/xxxxxxxxxx

Improvement of n-type conductivity in hexagonal boron nitride monolayer by doping, strain and adsorption

Yi-min Ding,[a] Jun-jie Shi,*[a] Min Zhang,[b] Xin-he Jiang,[a] Hong-xia Zhong,[a] Pu Huang,[a] Meng Wu[a] and Xiong Cao[a]

Received Date
Accepted Date

DOI: 10.1039/xxxxxxxxxx

www.rsc.org/journalname

The n-type conductivity of hexagonal boron nitride (*h*-BN) monolayer has been studied based on the state-of-the-art first-principles calculations. We adopt three different methods, such as C, S, Si and Si-*n*O (*n*=1,2,3) doping, strain and alkali metal (AM) atom (Li, Na, K and Rb) adsorption, to improve the n-type conductivity of *h*-BN monolayer. Three important results are obtained. First, as donor dopants, the activation energies (E_D) of C_B, S_N and Si_B are 1.22, 0.50 and 0.86 eV, respectively. The E_D of Si can be further reduced by the Si-*n*O codoping with increasing of O-atom number and decreases to 0.39 eV for Si-3O. Second, E_D can be effectively reduced by applying strain. The Si-3O has the lowest activation energy of 0.06 eV under the 4% compressive biaxial strain. Finally, there is an obvious charge transfer from the adsorbed AM atoms to *h*-BN monolayer, which results in an enhancement of electron concentration and improvement of n-type conductivity. This charge transfer is insensitive to the strain. The present results are significant to improve the performance of *h*-BN based two-dimensional optoelectronic nanodevices.

Keywords: *h*-BN monolayer; n-type doping; strain; alkali metal atom adsorption; first-principles calculations

1 Introduction

In recent years, two-dimensional (2D) materials have attracted much attention due to their unique physical properties and innovative device applications.[1,2] As one of the important members of 2D material family, hexagonal BN (*h*-BN) has been at the centre of the 2D material investigations for a long time. The *h*-BN monolayer or nanosheet has been synthesized by using different methods, such as ultrasonication of a hexagonal BN flake in dimethylformamide,[3] chemical vapor deposition (CVD),[4,5] liquid exfoliation,[6] mechanical exfoliation,[7] and low pressure CVD.[8] Similar to graphene, *h*-BN monolayer has a honeycomb structure and exhibits partly ionic B-N bond. This directly leads to a large band gap (~6 eV),[9] which allows *h*-BN monolayer to be used as an excellent candidate for nanoscale ultraviolet (UV) emisssion devices, such as UV light-emitting diodes (LEDs)[10] and laser diodes (LDs).[11] This unique structure leads to some excellent properties,[8] such as high chemical and thermal stabilities, enhanced thermal conductivity in the basal plane, and versatile doping capabilities. Hence *h*-BN nanosheets have been widely used in dielectric layers/substrates,[12] thermal management for electronic devices,[13] functional coatings,[14] UV photodetectors,[15] and neutron detectors.[16]

In order to improve the performance of *h*-BN based optoelectronic devices, we need stable and reproducible p-type and n-type *h*-BN materials. The p-type *h*-BN materials have been realised by doping of Zn,[17] Be[18] and Mg.[10] On the contrary, there have been even less reports on the growth and characterization of n-type *h*-BN film or monolayer. It was reported that carbon incorporation could induce n-type conduction of BN films in mixed cubic and hexagonal phases.[19] Wei *et al*.[20] found that the B atom in a BN monolayer could be replaced with C atom via electron-beam-induced doping, which results in n-type conductivity. However, the C_B was found to occupy preferentially the BN monolayer edges and the wrinkled domains. Both experiments[21] and theoretical calculations[22] confirmed that the doped carbon atoms segregate into isolated and irregularly shaped graphene islands embed in BN monolayer. A theoretical calculation further indicated that the substitution Si incorporated at a B site and O or S at a N site in *h*-BN bulk will act as donors and their donor activation energies (E_D) are 1.19, 0.33 and 1.22 eV, respectively.[23] Majety *et al*. reported that, as a n-type dopant, the E_D of Si is measured as 1.19 eV in *h*-BN films.[24] Obviously, these values

[a] *State Key Laboratory for Mesoscopic Physics and Department of Physics, Peking University, Beijing 100871, P.R. China. Fax: +86-10-62751615; Tel: +86-10-62757594; E-mail: jjshi@pku.edu.cn*

[b] *College of Physics and Electronic Information, Inner Mongolia Normal University, Hohhot 010022, P.R. China*

RSC Advances Accepted Manuscript

are too large to active the donor. Moreover, Tang *et al*. found that *h*-BN nanosheet can be converted into a n-type semiconductor by organic molecule adsorption.[25] However, the amount of the charges transferred from the organic molecules to the BN nanosheet is very small. We thus can see that it is still a great challenge for the synthesis of stable and reproducible n-type *h*-BN materials due to the high donor activation energy, phase separation and low transferring electron concentration from the adsorbed organic molecules, which greatly limits the widespread development and application of *h*-BN based optoelectronic devices.

Our purpose here is to explore three different methods (doping, strain and adsorption) to reduce the donor activation energy and improve the n-type conductivity of *h*-BN monolayer by using the advanced first-principles calculations. We find that Si-*n*O codoping can significantly reduce the donor activation energy. By applying a compressive strain, the donor activation energy can be reduced obviously. The charge transferred from adsorbed alkali metal (AM) atoms to *h*-BN monolayer can increase the electron concentration and thus improve the n-type conductivity.

2 Computational methods

Our calculations were performed by using density functional theory (DFT) in the generalized gradient approximation (GGA) with the Perdew-Burke-Ernzerhof (PBE) functional for electron exchange and correlation potentials as implemented in Vienna *ab initio* simulation package (VASP).[26,27] The electron-ion interaction was described by the projector augmented wave (PAW) method, and the energy cutoff was set to 450 eV. A 7×7 *h*-BN supercell was used in our calculations. The structures were fully optimised using the conjugate gradient algorithm until the residual atomic forces to be smaller than 0.01 eV/Å. The supercell with periodic boundary conditions was adopted to model the BN structures, with a vacuum layer larger than 18 Å to eliminate the interaction between the defects in the neighboring cells. A Γ-centered 5×5×1 *k*-point sampling was adopted. Convergence with respect to the cutoff energy and *k*-point sampling has been carefully checked.

In general, the formation energy E^{f} of a defect D in charge state q can be calculated as follows,[28]

$$E^{\mathrm{f}}[D(q)] = E_{\mathrm{tot}}[D(q)] - E_{\mathrm{tot}}[\mathrm{host}] - \sum_i n_i\mu_i + q(E_V + E_F + \Delta V[D]), \quad (1)$$

where $E_{\mathrm{tot}}[D(q)]$ is the total energy of the supercell containing the defect D in charge state q, E_{tot}[host] is the total energy in the same supercell without the defect, n_i is the atom number of the *i*th constituent, which has been added to (n_i>0) or removed from (n_i<0) the host material, and μ_i is its chemical potential. The Fermi level E_{F} is referenced to the valence band maximum (VBM) E_{V} of the host. The range of E_{F} is from VBM to conduction band minimum (CBM). A correction term $\Delta V[D]$ is introduced in order to align the electrostatic potential in the charged defect supercell with that in the host. The *h*-BN materials are usually grown under N-rich or N-poor conditions, which directly determines the type and concentration of defects. We thus consider these two limited cases to calculate the defect formation energy. For the N-rich condition, $\mu_{\mathrm{N}}=\mu_{\mathrm{N[N_2]}}$ (the energy of a N atom in N_2 molecule). For the N-poor condition, $\mu_{\mathrm{B}}=\mu_{\mathrm{B[bulk]}}$ (the energy of a B atom in α-rhombohedral phase of boron).

It is well-known that the traditional GGA method seriously underestimates the band gap values of semiconductors. This will directly induce errors in the defect formation energy and activation energy calculations. To overcome the band gap underestimation problem, several approaches have been proposed over the last few years.[29–31] Most of these approaches are based on an extrapolation of the results obtained by varying certain parameters that affect the band gap. One of the parameters which is usually utilised to do the extrapolation is the strain. By applying strain, one can compare the variation of the conduction band with respect to the valence band versus the variation of the defect level with respect to the conduction band.[32,33] The defect level position can then be extrapolated to the case corresponding to the experimental band gap through a comparison of the coefficient of the defect level versus strain with the coefficient of the bulk band gap versus strain,[34] *i.e.*,

$$\Delta E_{\mathrm{A}} = \frac{a^{\mathrm{def}}}{b^{\mathrm{bulk}}}\Delta E_{\mathrm{g}}, \quad (2)$$

where a^{def} and b^{bulk} are the rates at which the defect level and bulk band gap vary with strain, $\Delta E_g = E_g^{\mathrm{expt}} - E_g^{\mathrm{GGA}}$ and $\Delta E_{\mathrm{A}} = E_{\mathrm{A}}^{\mathrm{expt}} - E_{\mathrm{A}}^{\mathrm{GGA}}$. If we can get the experimental band gap E_g^{expt}, the activation energy corresponding to this gap value can also be obtained from eqn (2).

According to Table IV of ref. 35, we know that, for some important semiconductors, such as Si, Ge, GaAs, GaN and ZnO, the band-gap energies derived from the GGA-1/2 method (1.137, 0.70, 1.41, 3.52 and 3.29 eV) are in very good agreement with experiment (1.17, 0.66-0.74, 1.519, 3.507 and 3.4 eV) and GW calculations (0.95-1.10, 0.66-0.83, 1.40-1.70, 3.15-3.47 and 2.51-3.07 eV), though they are obtained at a computational cost comparable to the ordinary GGA. Moreover, Figs. 4 and 5 of ref. 36 also confirm that, compared with experiments, the GGA-1/2 calculation can give an accurate band gap for lots of materials with minimal computational effort. We thus use the band gap obtained from the GGA-1/2 calculations to replace the unavailable experimental value for the strained *h*-BN. In our calculations for the donor activation energy, only the band gaps are obtained by the GGA-1/2 method. The gap values are used in eqn (2) to calculate the difference of the experimental band gap and the GGA band gap. By giving the strain, we can get the rates at which the defect level and band gap vary with strain. Finally, the activation energy can be derived from eqn (2).

3 Results and discussion

3.1 Fundamental electronic structures of *h*-BN monolayer

To guarantee the accuracy of our calculated defect formation energy and donor activation energy, we first optimise the lattice parameters of *h*-BN monolayer on the basis of the minimization of the total energy and obtain $a=b=2.511$ Å, which are very close to the experimental values $a=b=2.51$ Å.[37] The electronic band structure and corresponding partial density-of-states (PDOS) cal-

RSC Advances Accepted Manuscript

This journal is © The Royal Society of Chemistry [year]

culated by using PBE functional show that *h*-BN monolayer has a direct band gap (~4.68 eV) and the VBM (CBM) of *h*-BN monolayer is mainly determined by the N-2*p* (B-2*p*) state. The top valence band width is 8.86 eV. These results are confirmed by the previous calculations.[38–40] Considering that the band gap is seriously underestimated in the usual GGA method, we thus adopt the GGA-1/2 method[35,36] to improve our calculations, in which the half ionization is applied to the *p*-orbital of N atom. We choose the trimming parameter $CUT=3.45$ (a.u.) and the power $n=2$ for N atom. This is because our calculated band gap with these parameters are 5.86 eV for *h*-BN monolayer shown in Fig. 1, which is in good agreement with the GW value (6.0 eV)[38] and the experimental value (6.0 eV).[9]

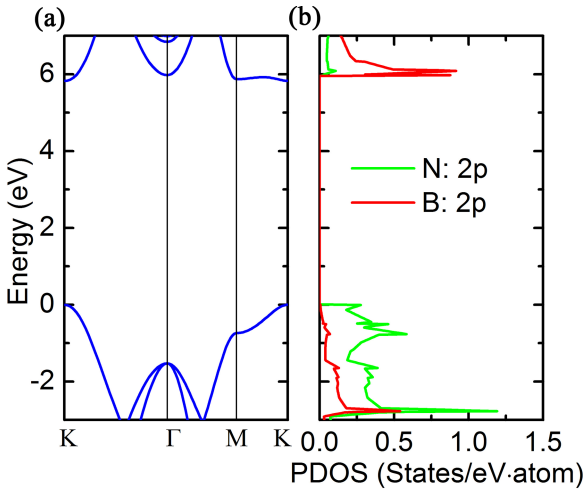

Fig. 1 The calculated electronic band structure (a) and the corresponding PDOS (b) for the *h*-BN monolayer. The energy band gap (E_g) derived from the GGA-1/2 calculation and the top valence band width are 5.86 and 8.86 eV, respectively. Our band-gap energy is close to the GW and experiment value of 6.0 eV.[9,38] The PDOSs of the N 2*s* and B 2*s* orbitals are small for the valence and conduction bands and have been neglected for clarity.

3.2 Doping of C, S, Si and Si-*n*O

It has been known that, as the commonly used donor dopants, C_B, S_N, Si_B and O_N are adopted to realise the n-type conductivity of *h*-BN bulk or films.[20,23,24] As a natural starting point for our purpose, *i.e.*, exploring the n-type doping strategy for *h*-BN monolayer, we would like to consider the donor-doping of C_B, S_N, Si_B and O_N in *h*-BN monolayer. Here, the doping means some host B or N atoms are replaced by other foreign atoms named as substitutional impurity. These impurity atoms, occupying the B or N positions, can remarkably modify the physical properties of the *h*-BN monolayer. Our calculated formation energies for C_B, S_N, Si_B and O_N are shown in Fig. 2. We can see from Fig. 2 that the donor activation energies (E_D) of C_B, S_N and Si_B are 1.22, 0.50 and 0.86 eV, respectively. This clearly shows that these dopants are not suitable for realising the n-type *h*-BN due to their large activation energies. For the O_N defect, we find that it is an amphoteric impurity, *i.e.*, a donor in p-type *h*-BN and an acceptor in n-type *h*-BN, which is similar to the behaviour of isolated interstitial hydrogen (H_i) in GaN.[28]

According to ref. 41, we know that codoping is a good method to reduce activation energy. We thus further calculate donor activation energy of Si-*n*O ($n=1,2,3$) complex. In order to find the preferable position of the O_N, we optimise the structure and calculate the total energy E_{tot} of *h*-BN:Si_B-O_N for the chosen four different positions (see inset of Fig. 3). We can see from Fig. 3 that E_{tot} increases monotonically from site 1 to 4. When O atom occupies position 1, E_{tot} of the supercell is the lowest and the corresponding structure becomes the most stable. This clearly shows that the Si-O bond is stronger than the Si-N bond. With increasing the number of O atoms, our structural optimisation proves that these O atoms are favourably distributed around the Si atom and the *h*-BN doped with Si-*n*O is still stable although the formation energy of the Si-*n*O complex is larger than that of C, S and Si donor dopants (see Fig. 2). The large defect formation energy just means that the corresponding defect is hard to form, which has no direct relation with the stability of the system. This can be understood as follows. It is well-known that the InN/GaN superlattice, grown by molecular-beam epitaxy (MBE) or metalorganic chemical vapor deposition (MOCVD) methods, is stable,[42] although it has a larger formation energy than the uniform $In_xGa_{1-x}N$ alloy with the same In concentration.[43,44] Moreover, the experiment also proves that the Si-B-O-N thin layer is stable.[45]

We know from our GGA calculations that the introduction of O atom can effectively reduce the activation energy (see Fig. 4a). The E_D decreases quickly with increasing of the O-atom number. For instance, E_D for Si-3O is reduced to 0.39 eV, which is 54.7% smaller than that of Si_B in *h*-BN. On the basis of extrapolation method, we further recalculate the activation energies of C, S, Si and Si-*n*O donor dopants in *h*-BN (see Table 1). We can see from Table 1 that the corrected donor activation energies by using GGA-1/2 method, increasing by about 0.3-0.5 eV on average, are in good agreement with the previous theoretical[23,46] and experimental[24] values. Generally, the donor activation energy obtained from GGA calculations is smaller than that from GGA-1/2 method. The physical reason is because of the underestimation of the band gap in the standard GGA calculations. The relative position of the donor level within the band gap can thus be moved if the band gap value is revised. Both GGA and GGA-1/2 calculations show that the donor activation energy of Si-*n*O complex can be reduced with increasing of the O-atom number.

In order to know the physical origin for the reduction of the donor activation energy, we systematically calculate the charge population (see Fig. 4b and Fig. 5) around the Si atom in the *h*-BN:Si-*n*O ($n=0,1,2,3$) by using the Bader charge analysis.[47–49] We can see from Fig. 4b and Fig. 5 that increasing of the O-atom number can lead to the increase of the Bader volume and the charge-density isosurface of the Si atom due to the strong Si-O bond. This means that Si atom transfers more electrons to its nearest neighbors and it will share a larger interaction region with the neighboring N and O atoms. The corresponding Si defect state thus becomes more delocalized due to the strong interaction between Si and its nearest O-atoms, which finally results in the reduction of the Si donor activation energy.[50]

RSC Advances Accepted Manuscript

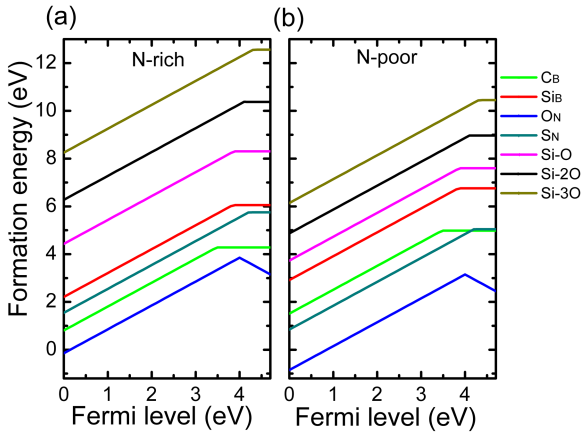

Fig. 2 Formation energy versus Fermi level for C_B, Si_B, S_N, O_N and Si-nO ($n = 1,2,3$) under N-rich (a) and N-poor (b) conditions.

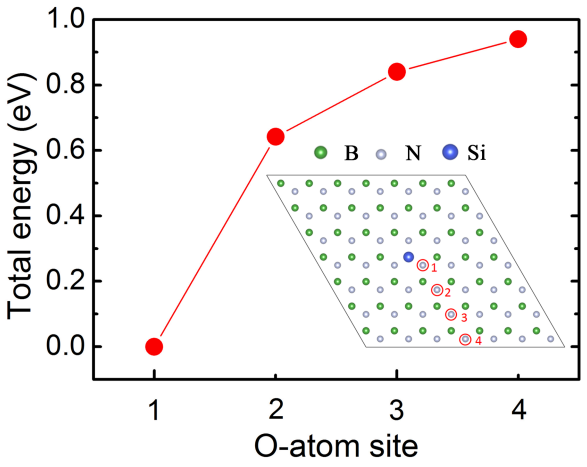

Fig. 3 The total energy of the Si_B-doped h-BN supercell with one O_N defect as a function of the O-atom site.

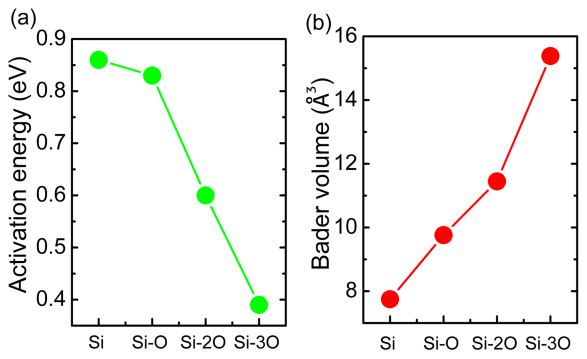

Fig. 4 (a) Activation energy of Si_B and Si-nO (n=1,2,3) complexes and (b) Bader volume of Si atom in the h-BN doped with Si_B or Si-nO defects.

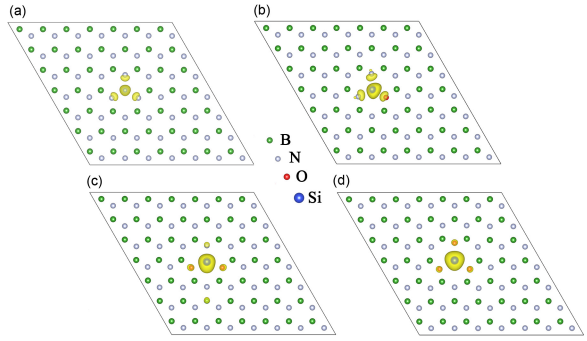

Fig. 5 The charge-density isosurface (ρ=0.01 eÅ^{-3}) of Si atom in h-BN:Si-nO (n=0,1,2,3). Here (a) is for Si atom, (b) for Si-O, (c) for Si-2O and (d) for Si-3O.

Table 1 Calculated donor activation energy E_D (in units of eV) by GGA and GGA-1/2 methods and some previous calculation[23,46] and experimental results[24]

Dopant	GGA	GGA-1/2	Previous result
C_B	1.22	1.67	1.55 [46]
S_N	0.50	1.04	1.22 [23]
Si_B	0.86	1.25	1.19 [23,24]
Si-O	0.83	1.12	
Si-2O	0.60	0.87	
Si-3O	0.39	0.65	

3.3 Strain effect

We calculate the donor activation energies (E_D) of C_B, Si_B, S_N and Si-3O doped in h-BN after applying biaxial strain, as shown in Fig. 6a. It can be seen that the activation energies of C_B, Si_B, S_N and Si-3O decrease slightly under the tensile strain and decrease obviously under the compressive strain. For example, the activation energies for C_B, Si_B, S_N and Si-3O decrease by 0.10, 0.28, 0.16 and 0.06 eV under 4% tensile strain, respectively. Moreover, their activation energies decrease by 0.41, 0.48, 0.40 and 0.34 eV under 4% compressive strain. We can see from Fig. 6a that the activation energies for S_N and Si-3O reduce to 0.09 and 0.06 eV under 4% compressive strain. A high electron concentration in the order of 10^{18} cm^{-3} can thus be expected. Considering the band gap correction from GGA-1/2 calculations, we further calculate the activation energies of C_B, Si_B, S_N and Si-3O (please refer to Fig. 6b) on the basis of eqn (2). Compared with the GGA results of Fig. 6a, we find that the extrapolated E_D values increase by about 0.3-0.5 eV on average. The tendency that the activation energy decreases slightly under the tensile strain and decreases obviously under the compressive strain is still valid. For the uniaxial strain case, our results are similar to the case of the biaxial strain (see Fig. 6c and d).

In order to analyse the physical reason of this reduction, we further calculate the GGA-1/2 revised energy gaps at K-K and K-Γ points as a function of the applied strain (see Fig. 7a and c). The energy gap between K-K points decreases as the strain increases, while the energy gap between K-Γ points increases as the strain increases. This conclusion is consistent with the previous work.[40] Under the compressive strain, the band gap decreases significantly, and the interaction between impurity and

RSC Advances Accepted Manuscript

This journal is © The Royal Society of Chemistry [year]

B/N atoms becomes stronger. The defect state thus becomes more delocalised, which will directly lead to the decrease of the donor activation energy E_D.[50] Under the tensile strain, the decrease of E_D is because of the moving-down of the CBM at K point (please refer to Fig. 7b and d).

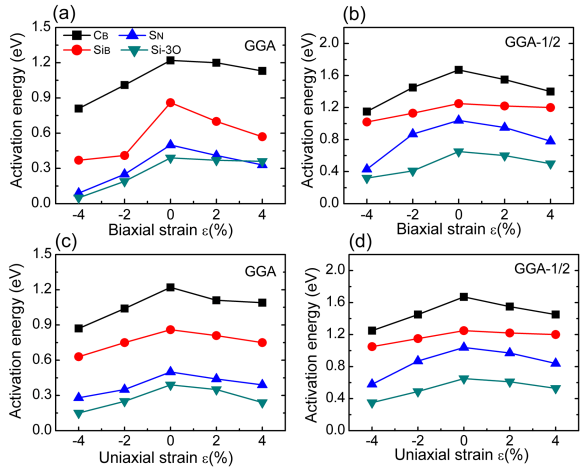

Fig. 6 Activation energy of C_B, Si_B, S_N and Si-3O doped in *h*-BN as a function of strain. Here (a) and (b) are for the biaxial strains, (c) and (d) for the uniaxial strains.

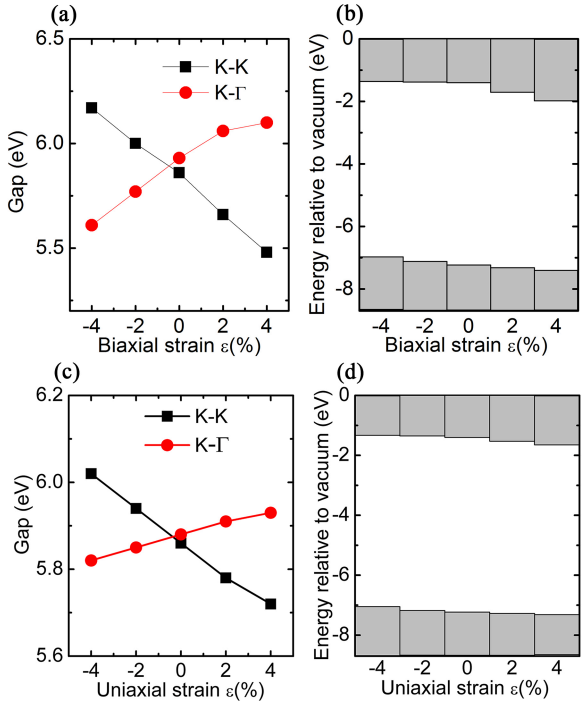

Fig. 7 The GGA-1/2 revised K-K energy gap and the K-Γ gap between VBM at K point and CBM at Γ point as a function of biaxial strain (a) and uniaxial strain (c). The calculated CBM and VBM alignment, relative to the vacuum level, for the different biaxial (b) and uniaxial (d) strain values.

3.4 Alkali metal atom adsorption

Generally, the 2D materials have the largest surface-to-volume ratio, and their surfaces are exposed to the exterior environment. Naturally, their surface properties can be easily manipulated by atom adsorption.[2] According to the difference of the interaction force between the adsorbed-atom and 2D material, the adsorption can be divided into physical and chemical adsorption. The physical adsorption means the interaction force between the adsorbed-atom and 2D material is the weak van der Waals force, in which no chemical bond is formed between them. On the contrary, if the combination of the adsorbed-atom and 2D material is due to the strong chemical bond, it is called the chemical adsorption, in which there is an obvious charge transfer between the adsorbed-atom and 2D material or the common charge owned by both.

Considering that the AM atoms are good potential donors due to their lowest ionisation energies and have been adsorbed on the graphite[51] and black phosphorene[52] to increase the concentration of free carriers, we thus investigate the adsorption of Li, Na, K and Rb atoms on *h*-BN monolayer and calculate their electronic structures, in which both the spin-polarised and non-polarised calculations are considered. We find that the same results are obtained for these two kinds of calculations. Our results (see Table 2) show that all the AM atoms favourably occupy the hollow site of hexagon and the elevation increases with the increasing of atomic radius from Li to Rb. According to Bader charge analysis, we can see that the AM atoms can give charge to BN monolayer and enhance its electron concentration. Particularly, the K-adsorbed *h*-BN monolayer has the smallest work function and K atom can thus give the most amount of charge because of the combining effect of the suitable elevation and ionisation energy of K atom. Here, the work function is defined as,

$$\Phi = E_{\mathrm{vac}} - E_{\mathrm{F}}, \tag{3}$$

where E_{vac} is the vacuum energy and E_{F} is the Fermi energy. The vacuum energy can be derived from the electrostatic potential in the z-direction away from the *h*-BN monolayer. The fundamental features of the band structures of *h*-BN monolayer adsorbed by Li, Na, K and Rb atoms are similar. From the typical band structures of the Li-atom absorbed on *h*-BN monolayer (see Fig. 8), we find the impurity bands approach the Fermi level at zero. These four AM atoms absorbed on *h*-BN monolayer behave as donor dopants and the n-type conductivity of *h*-BN monolayer can thus be improved.

Furthermore, by applying 4% tensile (compressive) strain, we find that the elevation decreases (increases) by approximately 1% (2%) and the charge transferred from the adsorbed AM atoms to *h*-BN monolayer increases (decreases) by about 1% (2%). The corresponding electronic band structure calculations show that the impurity bands still approach the Fermi level and the variations of both the conduction and valance band edges for the AM atom absorbed *h*-BN monolayer are similar to Fig. 7b and d.

4 Conclusions

In summary, we have investigated the n-type conductivity of the *h*-BN monolayer on the basis of first-principles calculations. In or-

RSC Advances Accepted Manuscript

Table 2 Elevation (H), transferred charge (Q) and work function (Φ) for the AM adatoms adsorbed on the hollow site in a *h*-BN monolayer

Atom	H (Å)	Q (*e*)	Φ (*eV*)
Li	3.38	0.13	2.71
Na	3.71	0.11	2.68
K	3.82	0.16	2.24
Rb	4.44	0.12	2.25

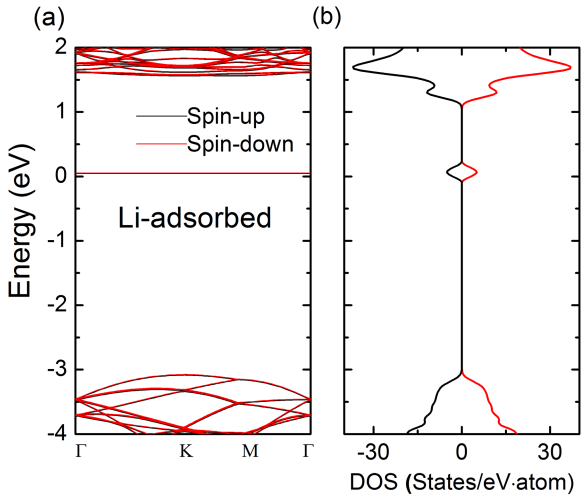

Fig. 8 The spin-polarised electronic band structure (a) and density of states (b) of Li-adsorbed *h*-BN monolayer. The impurity bands approach the Fermi level at zero.

der to enhance n-type conductivity, we adopt three different ways including monodoping and codoping, applying uniaxial and biaxial strain and AM atom adsorption. We find that C_B, S_N and Si_B are deep donors with donor activation energies of 1.22, 0.50 and 0.86 eV, respectively. Furthermore, Si-*n*O (n=1,2,3) codoping can greatly reduce the donor activation energy with increasing of the O-atom number. For the Si-3O doped *h*-BN monolayer, its activation energy decreases by 0.47 (54.7%) eV compared with the Si-doped case. The donor activation energies for these dopants can be reduced significantly under the condition of applying strain. The minimum activation energy 0.06 eV is obtained for Si-3O doped *h*-BN monolayer under the 4% compressive biaxial strain, which will lead to the high electron concentration in the order of 10^{18} cm^{-3}. The charges transferred from the adsorbed AM (Li, Na, K and Rb) atoms to *h*-BN monolayer, especially for K-atom with 0.16 e/per-atom, can improve the electron concentration, which is insensitive to the strain. The good n-type conductivity of *h*-BN monolayer, sensitively depending on both the donor activation energy and the electron concentration, can thus be expected. We hope that this work can stimulate further experimental investigations on the n-type *h*-BN monolayer and related optoelectronic nanodevices.

Acknowledgements

This work was supported by the Ministry of Science and Technology of the People's Republic of China (2012CB619304) and the National Natural Science Foundation of China (11474012, 11364030 and 11404013). We used computational resource of the "Explorer 100" cluster system of Tsinghua National Laboratory for Information Science and Technology.

References

1 F. Xia, H. Wang, D. Xiao, M. Dubey and A. Ramasubramaniam, *Nature Photon.*, 2014, **8**, 899-907.
2 S. Z. Butler, S. M. Hollen, L. Cao, Y. Cui, J. A. Gupta, H. R. Gutiérrez, T. F. Heinz, S. S. Hong, J. Huang, A. F. Ismach, E. Johnston-Halperin, M. Kuno, V. V. Plashnitsa, R. D. Robinson, R. S. Ruoff, S. Salahuddin, J. Shan, L. Shi, M. G. Spencer, M. Terrones, W. Windl and J. E. Goldberger, *ACS Nano*, 2013, **7**, 2898-2926.
3 C. Y. Zhi, Y. Bando, C. C. Tang, H. Kuwahara and D. Golberg, *Adv. Mater.*, 2009, **21**, 2889-2893.
4 R. Y. Tay, M. H. Griep, G. Mallick, S. H. Tsang, R. S. Singh, T. Tumlin, E. H. T. Teo and S. P. Karna, *Nano Lett.*, 2014, **14**, 839-846.
5 X. M. Li, J. Yin, J. X. Zhou and W. L. Guo, *Nanotechnology*, 2014, **25**, 105701.
6 P. Kumbhakar, A. K. Kole, C. S. Tiwary, S. Biswas, S. Vinod, J. Taha-Tijerina, U. Chatterjee and P. M. Ajayan, *Adv. Optical Mater.*, 2015, **3**, 828-835.
7 L. H. Li, E. G. Santos, T. Xing, E. Cappelluti, R. Roldan, Y. Chen, K. Watanabe and T. Taniguchi, *Nano Lett.*, 2015, **15**, 218-223.
8 J. Wang, Z. Wang, H. Cho, M. J. Kim, T. K. Sham and X. Sun, *Nanoscale*, 2015, **7**, 1718-1724.
9 K. K. Kim, A. Hsu, X. Jia, S. M. Kim, Y. Shi, M. Hofmann, D. Nezich, F. J. Rodriguez-Nieva, M. Dresselhaus, T. Palacios and J. Kong, *Nano Lett.*, 2012, **12**, 161-166.
10 H. X. Jiang and J. Y. Lin, *Semicond. Sci. Technol.*, 2014, **29**, 084003.
11 H. Jeong, S. Bang, H. M. Oh, H. J. Jeong, S.-J. An, G. H. Han, H. Kim, K. K. Kim, J. C. Park, Y. H. Lee, G. Lerondel and M. S. Jeong, *ACS Nano*, 2015, **9**, 10031-10038.
12 K. K. Kim, A. Hsu, X. Jia, S. M. Kim, Y. Shi, M. Dresselhaus, T. Palacios and J. Kong, *ACS Nano*, 2012, **6**, 8583-8590.
13 C. W. Chang, A. M. Fennimore, A. Afanasiev, D. Okawa, T. Ikuno, H. Garcia, D. Li, A. Majumdar and A. Zettl, *Phys. Rev. Lett.*, 2006, **97**, 085901.
14 A. Pakdel, C. Zhi, Y. Bando, T. Nakayama and D. Golberg, *ACS Nano*, 2011, **5**, 6507-6515.
15 Z. Q. Wu, X. Q. Li, H. K. Zhong, S. J. Zhang, P. Wang, T.-H. Kim, S. S. Kwak, C. Liu, H. S. Chen and S.-W. Kim, *Opt. Express*, 2015, **23**, 18864-18871.
16 J. Li, R. Dahal, S. Majety, J. Y. Lin and H. X. Jiang, *Nucl. Instrum. Methods Phys. Res. A*, 2011, **654**, 417-420.
17 K. Nose, H. Oba and T. Yoshida, *Appl. Phys. Lett.*, 2006, **89**, 112124.
18 B. He, W. J. Zhang, Z. Q. Yao, Y. M. Chong, Y. Yang, Q. Ye, X. J. Pan, J. A. Zapien, I. Bello, S. T. Lee, I. Gerhards, H. Zutz and H. Hofsäss, *Appl. Phys. Lett.*, 2009, **95**, 252106.
19 R. W. Pryor, *Appl. Phys. Lett.*, 1996, **68**, 1802-1804.

RSC Advances Accepted Manuscript

This journal is © The Royal Society of Chemistry [year]

20 X. L. Wei, M.-S. Wang, Y. Bando and D. Golberg, *ACS Nano*, 2011, **5**, 2916-2922.

21 P. Sutter, R. Cortes, J. Lahiri and E. Sutter, *Nano Lett.*, 2012, **12**, 4869-4874.

22 J. Martins and H. Chacham, *ACS Nano*, 2011, **5**, 385-393.

23 F. Oba, F. Togo, I. Tanaka, K. Watanabe and T. Taniguchi, *Phys. Rev. B: Condens. Matter Mater. Phys.*, 2010, **81**, 075125.

24 S. Majety, T. C. Doan, J. Li, J. Y. Lin and H. X. Jiang, *AIP Adv.*, 2013, **3**, 122116.

25 Q. Tang, Z. Zhou and Z. Chen, *J. Phys. Chem. C*, 2011, **115**, 18531-18537.

26 G. Kresse and J. Furthmüller, *Comp. Mater. Sci.*, 1996, **6**, 15-50.

27 G. Kresse and D. Joubert, *Phys. Rev. B: Condens. Matter Mater. Phys.*, 1999, **59**, 1758-1775.

28 C. G. Van de Walle and J. Neugebauer, *J. Appl. Phys.*, 2004, **95**, 3851-3879.

29 S. B. Zhang, S. H. Wei and A. Zunger, *Phys. Rev. B: Condens. Matter Mater. Phys.*, 2001, **63**, 075205.

30 S. B. Zhang, *J. Phys.: Condens. Matter*, 2002, **14**, R881-R903.

31 A. Janotti and C. G. Van de Walle, *Appl. Phys. Lett.*, 2005, **87**, 122102.

32 I. Gorczyca, A. Svane and N. E. Christensen, *Solid State Commun.*, 1997, **101**, 747-752.

33 A. Janotti, S. B. Zhang, S. H. Wei and C. G. Van de Walle, *Phys. Rev. Lett.*, 2002, **89**, 086403.

34 C. Freysoldt, B. Grabowski, T. Hickel, J. Neugebauer, G. Kresse, A. Janotti and C. G. Van de Walle, *Rev. Mod. Phys.*, 2014, **86**, 253-305.

35 L. G. Ferreira, M. Marques and L. K. Teles, *Phys. Rev. B: Condens. Matter Mater. Phys.*, 2008, **78**, 125116.

36 L. G. Ferreira, M. Marques and L. K. Teles, *AIP Adv.*, 2011, **1**, 032119.

37 L. Liu, Y. P. Feng and Z. X. Shen, *Phys. Rev. B: Condens. Matter Mater. Phys.*, 2003, **68**, 104102.

38 X. Blase, A. Rubio, S. G. Louie and M. L. Cohen, *Phys. Rev. B: Condens. Matter Mater. Phys.*, 1995, **51**, 6868-6875.

39 Z. Y. Huang, C. Y. He, X. Qi, H. Yang, W. L. Liu, X. L. Wei, X. Y. Peng and J. X. Zhong, *J. Phys. D: Appl. Phys.*, 2014, **47**, 075301.

40 Y. Fujimoto, T. Koretsune and S. Saito, *J. Ceram. Soc. Jpn.*, 2014, **122**, 346-348.

41 H.-X. Zhong, J.-J. Shi, M. Zhang, X.-H. Jiang, P. Huang and Y.-M. Ding, *AIP Adv.*, 2015, **5**, 017114.

42 M. E. Lin, F. Y. Huang and H. Morkoc, *Appl. Phys. Lett.*, 1994, **64**, 2557-2559.

43 S. Zhang, J.-J. Shi, S.-G. Zhu, F. Wang, M. Yang and Z.-Q. Bao, *Phys. Lett. A*, 2010, **374**, 4767-4773.

44 J. Z. Liu and A. Zunger, *Phys. Rev. B: Condens. Matter Mater. Phys.*, 2008, **77**, 205201.

45 G. Wen, G. L. Wu, T. Q. Lei, Y. Zhou and Z. X. Guo, *J. Eur. Ceram. Soc.*, 2000, **20**, 1923-1928.

46 B. Huang and H. Lee, *Phys. Rev. B: Condens. Matter Mater. Phys.*, 2012, **86**, 245406.

47 G. Henkelman, A. Arnaldsson and H. Jonsson, *Comp. Mater. Sci.*, 2006, **36**, 354-360.

48 E. Sanville, S. D. Kenny, R. Smith and G. Henkelman, *J. Comput. Chem.*, 2007, **28**, 899-908.

49 W. Tang, E. Sanville and G. Henkelman, *J. Phys.: Condens. Matter.*, 2009, **21**, 084204.

50 M. F. Li, *Modern Semiconductor Quantum Physics*, World Scientific Publishing Company, Singapore, 1995.

51 M. Caragiu and S. Finberg, *J. Phys.: Condens. Matter*, 2005, **17**, 995-1024.

52 T. Hu and J. Hong, *J. Phys. Chem. C*, 2015, **119**, 8199-8207.

RSC Advances Accepted Manuscript

Table of Contents Entry

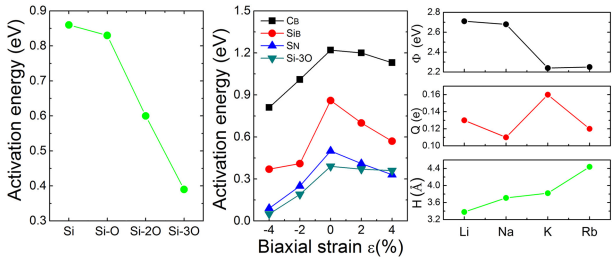

The n-type conductivity of *h*-BN monolayer is improved significantly by doping, strain and alkali-metal atom adsorption.

RSC Advances Accepted Manuscript

This journal is © The Royal Society of Chemistry [year]